

Design of coherent receiver optical front end for unamplified applications

Bo Zhang,* Christian Malouin, and Theodore J. Schmidt

Juniper Networks, 1194 N. Mathilda Ave. Sunnyvale, California 94089, USA

*bozhang@juniper.net

Abstract: Advanced modulation schemes together with coherent detection and digital signal processing has enabled the next generation high-bandwidth optical communication systems. One of the key advantages of coherent detection is its superior receiver sensitivity compared to direct detection receivers due to the gain provided by the local oscillator (LO). In unamplified applications, such as metro and edge networks, the ultimate receiver sensitivity is dictated by the amount of shot noise, thermal noise, and the residual beating of the local oscillator with relative intensity noise (LO-RIN). We show that the best sensitivity is achieved when the thermal noise is balanced with the residual LO-RIN beat noise, which results in an optimum LO power. The impact of thermal noise from the transimpedance amplifier (TIA), the RIN from the LO, and the common mode rejection ratio (CMRR) from a balanced photodiode are individually analyzed via analytical models and compared to numerical simulations. The analytical model results match well with those of the numerical simulations, providing a simplified method to quantify the impact of receiver design tradeoffs. For a practical 100Gb/s integrated coherent receiver with 7% FEC overhead, we show that an optimum receiver sensitivity of -33dBm can be achieved at GFEC cliff of $8.55\text{E-}5$ if the LO power is optimized at 11dBm . We also discuss a potential method to monitor the imperfections of a balanced and integrated coherent receiver.

©2012 Optical Society of America

OCIS codes: (060.0060) Fiber optics and optical communications; (060.2380) Fiber optics sources and detectors.

References and links

1. S. J. Savory, "Digital coherent optical receivers: algorithms and subsystems," *IEEE J. Sel. Top. Quantum Electron.* **16**(5), 1164–1179 (2010).
2. M. Birk, P. Gerard, R. Curto, L. E. Nelson, X. Zhou, P. Magill, T. J. Schmidt, C. Malouin, B. Zhang, E. Ibragimov, S. Khatana, M. Glavanovic, R. Lofland, R. Marcocchia, R. Saunders, G. Nicholl, M. Nowell, and F. Forghieri, "Real-time single-carrier coherent 100 Gb/s PM-QPSK field trial," *J. Lightwave Technol.* **29**(4), 417–425 (2011).
3. G. P. Agrawal, *Fiber-optic Communication Systems*, 3rd ed. (John Wiley & Sons, Inc., 2002).
4. K. Kikuchi, "Coherent optical communication systems," in *Optical Fiber Telecommunications, V*, I. P. Kamniov, T. Li and A. E. Willner, eds. (Elsevier, 2008), Vol. B. Chap. 3.
5. C. R. Doerr, L. Zhang, P. J. Winzer, N. Weimann, V. Houtsma, T. Hu, N. J. Sauer, L. L. Buhl, D. T. Neilson, S. Chandrasekhar, and Y. K. Chen, "Monolithic InP dual-polarization and dual-quadrature coherent receiver," *IEEE Photon. Technol. Lett.* **23**(11), 694–696 (2011).
6. Y. Painchaud, M. Poulin, M. Morin, and M. Têtù, "Performance of balanced detection in a coherent receiver," *Opt. Express* **17**(5), 3659–3672 (2009).
7. A. Carena, V. Curri, P. Poggiolini, and F. Forghieri, "Dynamic range of single-ended detection receivers for 100 GE coherent PM-QPSK," *IEEE Photon. Technol. Lett.* **20**(15), 1281–1283 (2008).
8. B. Razavi, *Design of Integrated Circuits for Optical Communication Systems* (McGraw-Hill, 2003).
9. OIF IA # OIF-DPC-RX-01.0, "Implementation agreement for integrated dual polarization intradyne coherent receivers," April 16, 2010.
10. C. Xie, "Local oscillator phase noise induced penalties in optical coherent detection systems using electronic chromatic dispersion compensation," in *Proceedings of OFC/NFOEC*, paper OMT4 (2009).

1. Introduction

With the ever increasing demand in transporting, routing and switching high-bandwidth data, modern telecommunication systems at 100-Gb/s or beyond are employing coherent detection technologies coupled with complex photonic modulation formats to satisfy the high spectral efficiency and reach requirements of modern DWDM transport systems [1,2]. By linearly down converting the amplitude, phase, and polarization of the modulated lightwave carrier into the electrical baseband, fiber transmission impairments, such as chromatic dispersion (CD) and polarization mode dispersion (PMD), can be effectively mitigated through sophisticated signal processing in the digital domain [1].

Stepping back two decades, the original motivation for coherent technologies was its inherent high sensitivity [3,4], utilizing a local oscillator (LO) laser to provide gain to the weak received signal. However, an alternate technology, the Erbium Doped Fiber Amplifier (EDFA) achieved the same goal while also providing a means to amplify the signal independent of the Rx location [4]. The EDFA ushered in a new era of fiber-optic communications and explorations on coherent reception were largely put on hold until the early 2000s. Modern research into coherent detection is primarily focused on amplified links, where the accumulation of amplified spontaneous emission (ASE) noise in optically amplified links negates much of the sensitivity benefit from utilizing a coherent receiver. The benefit of coherent detection in these applications is, instead, the powerful impairment mitigation through digital signal processing [1]. While optically-amplified links are currently the primary focus for coherent research and development, coherent detection also provides a powerful means to provide high bandwidth services over unamplified fiber-optic links that cannot be accomplished via traditional means (e.g. 100G over 80 + km). The high symbol rates and complex photonic modulation formats required to meet the bandwidth requirements of modern networks present new challenges for system designers and require a fundamental understanding of the practical limitations of receiver sensitivity using modern coherent receivers.

Driven by the size, power and cost requirements, integrated photonics technology plays an ever-increasing role in modern fiber-optic transport systems [5]. Photonic integration puts practical limits on achievable sensitivity in coherent receivers, as each individual component exhibits non-ideal characteristic which introduces a non-negligible noise floor.

In this paper, we first review the various noise sources present in a coherent receiver front end. We then show, via an analytical model, that the sensitivity is optimized when the input-referred thermal noise is equal to the LO-RIN beat noise suppressed by the CMRR of the coherent mixer. This is shown to result in an optimum LO power for a given integrated receiver design. The analytical models are shown to produce results consistent with numerical simulation and are used to predict the impact and dependencies of various noise sources on system performance. We show that an optimum receiver sensitivity of -33dBm can be achieved for a practical 100Gb/s (with 7% FEC overhead) integrated coherent receiver front end when the LO power is optimized at 11dBm. We finally discuss a potential method to monitor the imperfections of a fully integrated balanced coherent receiver.

2. Noise sources in coherent receivers

Figure 1 shows a typical polarization-diverse coherent receiver, consisting of a free running local oscillator (LO), two polarization beam splitters (PBSs), two 90 degree hybrid mixers to decompose the in-phase and quadrature channels, and four sets of balanced photodiodes (PDs) followed by four differential transimpedance amplifiers (TIAs). Balanced detection is assumed for its superior common mode suppression properties, as opposed to single-ended detection schemes [6]. Furthermore, balanced detection typically requires less LO power and greatly enhances the input signal dynamic range [7].

For unamplified link applications, one assumes the received optical signal is free of optical noise, and thus the noise generated from the coherent receiver dominates the ultimate receiver sensitivity. Shot noise and thermal noise are the two fundamental noise mechanisms responsible for current fluctuations in an optical receiver, even when the incident optical power is constant.

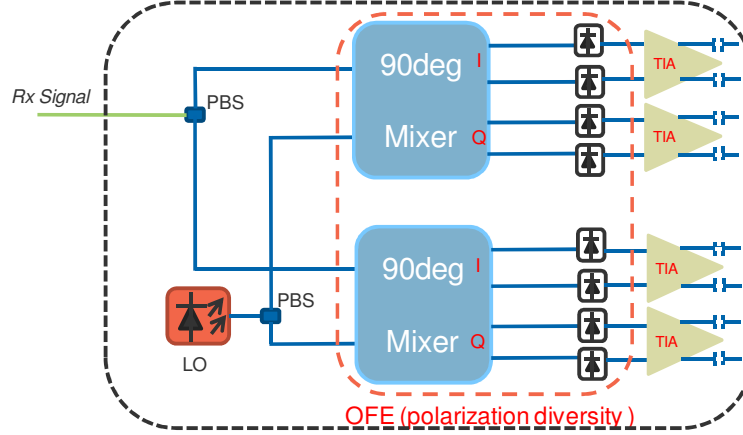


Fig. 1. Block diagram of a fully-integrated optical coherent receiver. LO: local oscillator; PBS: polarization beam splitter; OFE: optical front end, which contains two 90 degree hybrid mixers and four sets of balanced photodiodes. TIA: transimpedance amplifier.

Shot noise is a manifestation of the fact that an electric current consists of a stream of electrons that are generated at random times [3]. It is a stationary random process which is usually approximated by Gaussian statistics. The one-sided shot noise power spectral density for each PD is normally expressed as follows,

$$\sigma_{shot}^2 = 2 * q * (\mathfrak{R} * P + I_d) * \Delta f \quad (1)$$

where q is the electron charge, \mathfrak{R} is the PD responsivity in Amps/Watts, P is the total power hitting the receiver and I_d is the dark current. Δf is the one-sided *effective noise bandwidth* of the receiver. For the high LO power and low input signal power conditions relevant to our sensitivity analysis, the total power can be approximated by the LO power alone. Two things are evident for shot noise in a coherent receiver. (1), it is linearly dependent on the LO power; (2), four sets of balanced receivers independently add uncorrelated shot noise of their own onto the overall incident signal.

Thermal noise is due to random thermal motion of electrons in a resistor, manifesting as a fluctuating current even in the absence of an applied voltage [3]. The load resistor in the front end of an optical receiver adds such fluctuations to the current generated by the PD. Usually, noise generated by the transimpedance amplifiers is the dominating thermal noise term and the amount added depends on the front-end design [8]. A simple approach to account for the thermal noise is to use the equivalent TIA input-referred noise current density [8], which relates to the thermal noise as follows,

$$\sigma_{TIA}^2 = (i_{TIA})^2 * \Delta f \quad (2)$$

where i_{TIA} is the one-sided differential input noise current density, expressed in $\frac{pA}{\sqrt{Hz}}$.

A third important noise term comes from the relative intensity noise (RIN) of the LO. This is due to the fact that the output of a semiconductor laser exhibits inevitable intensity fluctuations from spontaneous emission even when it is biased at a constant current [3]. For coherent receivers, the beating between the LO and its intensity noise acts as an interference

term onto the useful signal-LO beat note. The LO-RIN beat noise variance on each of the eight PDs can be expressed as follows,

$$\sigma_{RIN}^2 = \mathfrak{R}^2 * P_{LO}^2 * (RIN) * 2\Delta f \quad (3)$$

where RIN is usually defined as a double-sided noise spectral density expressed in dB/Hz, when translated into a logarithmic scale. There are several things worth noting in Eq. (3). First, the noise variance is quadratically dependent on the LO power. Second, the noise variance is on each individual PD and is well correlated between P and N ports in each of the four tributaries. Third, for ideal balanced detection, this interference term will be completely rejected. However, due to imperfect balancing, the LO-RIN beat noise will be suppressed by a finite rejection ratio. The residual will leak through and act as a non-negligible interference term, especially when the LO power is high. The amount of leakage is determined by the balanced mixer's common mode rejection ratio (CMRR), which is the subject of the next section.

Additional imperfections can exist in a coherent receiver, such as I/Q tributary power imbalances, quadrature phase errors, and delay mismatches, X/Y channel power imbalances, and delay mismatches. Fortunately, these non-idealities are captured in the digitized waveforms on the four tributaries and can, in theory, be mitigated by modern DSP technologies. On the other hand, the P/N level imperfections (described in the next section) are embedded in the waveforms once the common mode subtraction is done and are difficult, if not impossible, to be compensated by signal processing techniques.

3. Imperfections in balanced mixers

If the received signal and the LO are equally split and synchronized from the last 2x2 coupler inside the 90 degree hybrid to each set of balanced PD, perfect cancellation of the common mode can be achieved. In reality, power imbalance and skew mismatch leads to a finite CMRR. Power imbalance can result from deviations in a 50/50 splitting ratio from the last coupler as well as unequal responsivities of the PDs. Skew mismatches are due to the P and N path length differences from the output of the last 2x2 coupler to the two inputs of the balanced PD. If we define the CMRR as the power ratio of the residual common mode with respect to the combined common mode [9], and translate into the frequency domain, one can write the CMRR of a balanced mixer as follows,

$$CMRR(f) = \left| \frac{\alpha^2 - e^{j2\pi f\tau}}{\alpha^2 + 1} \right|^2 \quad (4)$$

where α is the splitting ratio of either the signal port or the LO port to the four sets of balanced PDs, and τ is the P/N skew of the four tributaries. One can see from the above equation that at low frequencies, CMRR is dictated by the power imbalance, whereas the skew determines the frequency dependent behavior of the CMRR [6].

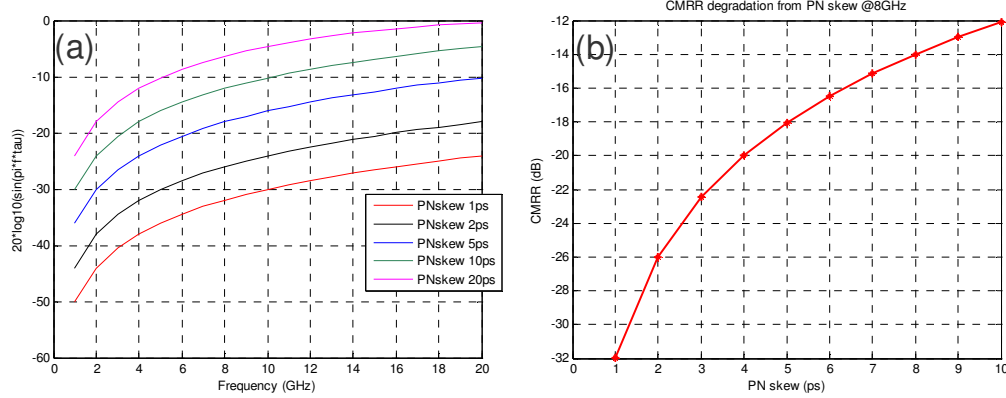


Fig. 2. (a) CMRR as a function of frequency for various P/N skew levels. Here, the power splitting ratio is assumed to be equal between P and N ports to magnify the frequency dependent nature of the CMRR. (b) Effective CMRR value as a function of P/N skew. The effective value is extracted from (a) at 8GHz for each skew level.

To explore the CMRR as a function of frequency, we assume equal power splitting by setting α equals 1. Equation (4) degenerates as follows on the log scale,

$$CMRR(f) = 20 * \log_{10}[\sin(2\pi f \tau)] \quad (5)$$

Figure 2(a) plots the CMRR degradation as a function of the frequency for various P/N skew values. We can see that for a 2-ps skew mismatch, the CMRR degrades by more than 20dB across the 20GHz frequency span.

To analytically quantify the CMRR impact on the amount of residual LO-RIN beat noise, it is beneficial to use a single value to represent an averaged CMRR. We choose CMRR at 8 GHz for our subsequent system-level simulation. This is based on the 16~20GHz analogue receiver bandwidth as well as the frequency dependent shape of the CMRR. Effective CMRR as a function of P/N skew is thus plotted in Fig. 2(b). For a 2ps P/N skew, -26dB represents the effective CMRR which can be used to calculate analytically the residual LO-RIN beat noise.

4. Theory for receiver sensitivity optimization

With the understanding of the various noise sources and the definition of the effective CMRR, we analytically derive the optimum receiver sensitivity by examining the beating notes for any of the four tributaries. The current at port P and port N of any of the four balanced photo-detectors can be represented as follows,

$$I_p(t) = \left[E_{SIG}(t) + [E_{LO} + E_{LO_IN}(t)] \right]^2 + i_{TIA} + i_{shot} \quad (6)$$

$$I_n(t + \tau) = \left[E_{SIG}(t + \tau) - [E_{LO} + E_{LO_IN}(t + \tau)] \right]^2 + i_{TIA} + i_{shot} \quad (7)$$

where E_{SIG} , E_{LO} , and E_{LO_IN} are the electric fields of the signal, LO and LO intensity noise, measured at the input to the PD, respectively. Note that the noise-free E_{LO} contains constant amplitude, whereas the LO intensity noise E_{LO_IN} bears the time-varying amplitude noise. Both terms can be considered to have the synchronous phase noise. τ represents the path length mismatch between the P and N ports. Both the signal and the LO intensity noise on the P and N ports are correlated with this skew difference. i_{TIA} is the thermal noise current from the TIA, and i_{shot} is the shot noise current from the PD. Both of these two noise terms on the P and N ports are uncorrelated and thus will be doubled after balanced detection.

After balanced current subtraction, the signal to noise ratio (SNR) at the output of the balanced PD (i.e., at the input to the differential TIA) is shown below,

$$SNR_{Rx_out} = \frac{\frac{1}{2} * 16 * \mathfrak{R}^2 * P_{LO} * P_{SIG}}{\sigma_{TIA}^2 + 16 * \mathfrak{R}^2 * P_{LO} * P_{LO_IN} * CMRR + \sigma_{shot}^2} \quad (8)$$

where P_{SIG} , P_{LO} , and P_{LO_IN} are the optical power of the signal, LO and LO intensity noise, measured at the input to the PD, respectively. The numerator is the useful signal-LO beat term and the $\frac{1}{2}$ factor accounts for the asynchronous phase noise from the signal and LO. The denominator has three noise variance terms, the thermal noise from the differential TIA, the doubled shot noise from the balanced PDs and the synchronous LO-RIN beat noise which is suppressed by the CMRR of the coherent mixer.

The receiver sensitivity cannot be directly derived from the above SNR_{Rx_out} equation as the useful signal power is not only amplified by the LO power, but also affected by the PD responsivity and the insertion loss of the 90 degree hybrid mixer. In order to directly read the sensitivity from the SNR representation, we introduce the concept of *coherent receiver input-referred noise variances*, as shown in the following equation,

$$SNR_{Rx_in} = \frac{P_s}{\sigma_{TIA_Rx_in}^2 + \sigma_{RIN_Rx_in}^2 + \sigma_{shot_Rx_in}^2} \quad (9)$$

The SNR_{Rx_in} has a numerator which is normalized to be exactly the received signal input power. The denominator contains three coherent receiver input-referred noise variances, which are explicitly expressed in Eq. (10). The factor 8 in front of the TIA noise accounts for the intrinsic 9dB loss using polarization- and phase-diversity, whereas the EL is the excess loss of the coherent mixer in linear scale. For simplicity, the excess loss from the signal port to the PD and the LO port to the PD are assumed the same.

$$SNR_{Rx_in} = \frac{P_s}{\frac{8 * (i_{TIA})^2 * \Delta f * EL^2 / \mathfrak{R}^2}{P_l} + P_l * 2 * (RIN * 2 * \Delta f) * CMRR + 2 * q * (2 * \Delta f) * EL / \mathfrak{R}} \quad (10)$$

Equation (10) can be written in a compact format in Eq. (11) which will reveal some important observations.

$$SNR_{Rx_in} = \frac{P_s}{\frac{THERMAL}{P_l} + P_l * LOIN * CMRR + SHOT} \quad (11)$$

$$THERMAL = 8 * (i_{TIA})^2 * \Delta f * EL^2 / \mathfrak{R}^2 \quad (12)$$

$$LOIN = 2 * (RIN * 2 * \Delta f) \quad (13)$$

$$SHOT = 2 * q * (2 * \Delta f) * EL / \mathfrak{R} \quad (14)$$

By referencing the noise terms to the input of the coherent receiver, shot noise (SHOT, Eq. (14)) is no longer dependent on the LO power and shows up as a constant noise floor. Whereas the originally constant thermal noise (THERMAL, Eq. (12)) floor is now inversely proportional to the LO power. The input-referred residual LO-RIN beat (LOIN, Eq. (13)) is now linearly proportional to the LO power. Since the total noise variance solely determines the SNR for a given input signal power level, one can see that there exist an optimal LO power which minimizes the total noise variances and thus maximize the SNR. This optimal LO power can be concisely expressed in log scale as follows,

$$P_{l_optimum} = \frac{1}{2} * (THERMAL - LOIN - CMRR) \quad (15)$$

Equation (15) shows that the optimum LO power, which is independent of shot noise, is obtained when the THERMAL noise is balanced with the LOIN suppressed by the CMRR.

5. Numerical simulations

Numerical simulations are carried out in Matlab to validate the above analytical model. 112.8Gb/s (28.2GBaud) non-return-to-zero polarization multiplexed quadrature phase shift keyed (NRZ-PM-QPSK) modulated signal is generated with 2^{19} pseudo random bit sequence (PRBS) length on each of the four tributaries. The coherent receiver contains a 100KHz linewidth local oscillator (LO) with a programmable RIN value in dB/Hz. The two 90 degree hybrids are modeled to have perfect I/Q and X/Y level balance, whereas the P/N skew represents the source of imperfection. Excess loss from the hybrid is assumed to be 1dB and the PD responsivity is set at 0.75A/W. Thermal noise is modeled to have a varying differential TIA input noise current density in pA/sqrt(Hz). The overall receiver analog bandwidth is modeled as having a 3dB bandwidth of 16GHz with a 5th order Butterworth shape. The 2 samples/symbol analog-to-digital converter (ADC) has an effective number of bits (ENOB) of 6, which is close to an ideal parameter. A 2x2 butterfly adaptive equalizer is realized in the frequency domain with LMS algorithm. Viterbi-viterbi based carrier phase estimation is performed to compensate for the phase noise. Error counting is performed to calculate the bit-error-rate (BER) and then converts to Q^2 factor to quantify the system performance. The following subsections evaluate separately the impact of LO RIN, thermal noise and CMRR respectively. We show that the analytical models presented in the previous section matches very well with the numerical simulations.

Unless explicitly stated, the numerical simulations are based on the following parameters in a nominal condition. ($i_{TIA} = 18.2 \frac{pA}{\sqrt{Hz}}$; $\Delta f = 20GHz$; $EL = 1dB$; $\mathfrak{R} = 0.75A/W$; $RIN = -145dB/Hz$; $\tau = 2ps$). This results in the following equivalent noise floors using Eqs. (12) to (14). THERMAL = -38.3 (dBm*dBm); LOIN = -35.97 (dB); CMRR = -26 (dB); SHOT = -46.68 (dBm). Note the various units for each term as THERMAL is proportional to Watts squared, SHOT is proportional to Watts. Both LOIN and CMRR are relative values.

5.1 Impact of LO RIN

We first analyze the impact of the relative intensity noise (RIN) from the LO. Figure 3(a) shows that for a given RIN value, there exists an optimum LO power which optimizes the system performance, in this example for a received signal power of -33dBm. For a RIN value of -145dB/Hz, the optimum LO power is approximately 11dBm. With other parameters unchanged, only increasing or decreasing the RIN value by 5dB correspondingly lowers or increases the optimum LO power by approximately 2.5dB, which matches well with the prediction from Eq. (15). At low LO power, system performance is more dominated by the thermal noise effect and thus shows less and less dependence on the RIN values. Please note that the Q penalties in Fig. 3(a) are relative to the optimum performance when the RIN is in the case of -150dB/Hz. With an optimum LO power of 13dBm, the Q value is 11.2dB.

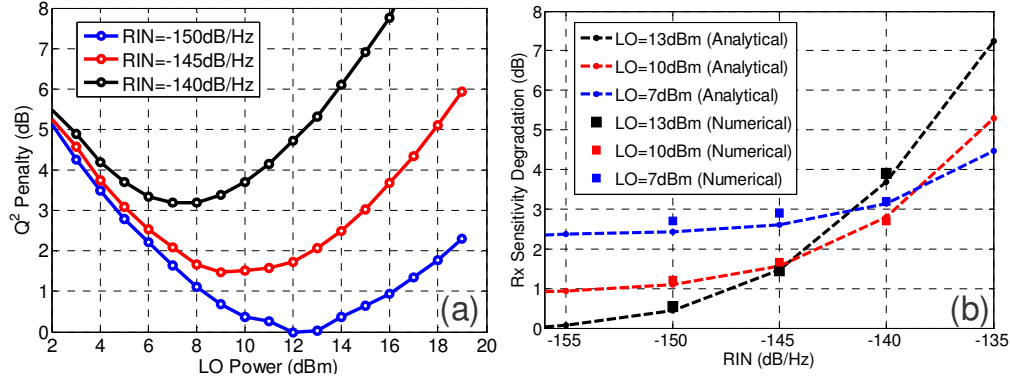


Fig. 3. (a) Numerical simulation of Q Penalty as a function of LO power for various LO RIN values. (b) Receiver sensitivity degradation versus RIN for various LO powers. The numerical simulation and analytical equations are seen to be in good agreement.

Figure 3(b) shows that for a given thermal noise level, receiver performance is actually more tolerant to the RIN values in the range of -155 to -135 dB/Hz, when the LO power is lowered. Note that the baseline performance is sacrificed by several dB with a reduced LO power.

5.2 Impact of thermal noise

Thermal noise from the differential TIA is then analyzed. Setting the received signal power at -33 dBm, Fig. 4(a) shows that for a given TIA noise current density, there exists an optimum LO power which optimizes the receiver performance. For a typical TIA noise current value of 18 pA/sqrt(Hz), the optimum LO power is around 11 dBm. With other parameters fixed, only increasing or reducing the TIA noise current density by a factor of 1.8 correspondingly increases or decreases the optimum LO power by exactly 2.5 dB, which matches well with the prediction from Eq. (15). At high LO power, the performance is more dominated by the residual LO RIN beat noise and thus shows less dependence on the TIA noise currents in the density range of interest.

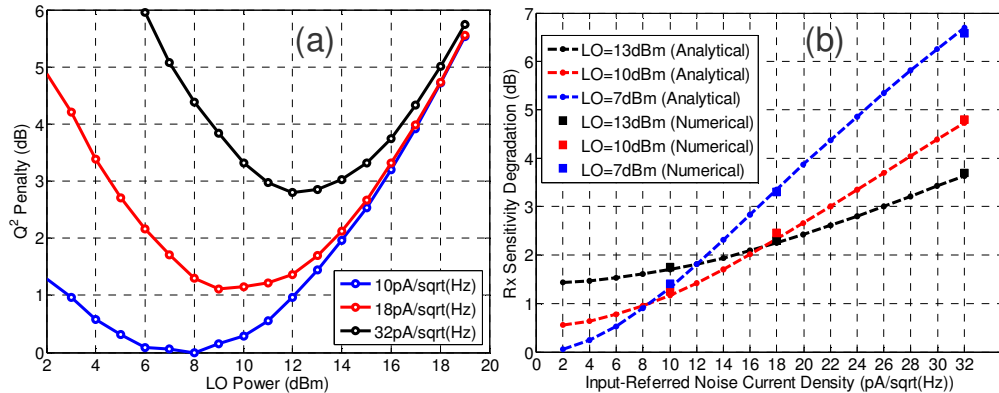


Fig. 4. (a) Numerical simulation of Q Penalty as a function of LO power for various TIA thermal values. (b) Receiver sensitivity degradation versus differential TIA input-referred noise current density for various LO powers. The numerical simulation and analytical equations are seen to be in good agreement.

Figure 4(b) shows that for a given RIN level, system performance is significantly less sensitive to thermal noise, in the range of 2 to 32 pA/sqrt(Hz), for higher LO power (13 dBm in

this example). However, the baseline sensitivity is reduced by several dB. Numerical simulations are seen to be in close agreement with the prediction from the analytical model.

5.3 Impact of CMRR

We finally study the impact of CMRR on the performance of a coherent receiver in unamplified applications.

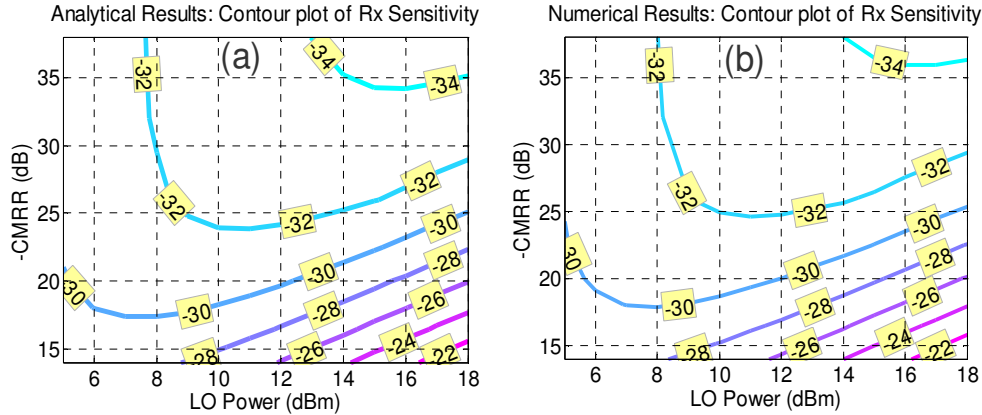


Fig. 5. (a) Analytical model predictions on the coherent receiver sensitivity at $8.55\text{e-}5$ BER as a contour plot against CMRR and LO power. (b) Numerical simulations on the coherent receiver sensitivity at $8.55\text{e-}5$ BER as a contour plot against CMRR and LO power.

In simulation, the P/N skew is swept from 0ps to 8ps in steps of 1ps. An effective CMRR is extracted based on the CMRR value at 8GHz. Figure 5 provides a contour map of the receiver sensitivity at $8.55\text{E-}5$ BER (GFEC cliff) as a function of effective CMRR (Y axis) and LO power (X axis) for nominal thermal noise and RIN values provided earlier in this section. The numerical simulation and the analytical model are again seen to be in excellent agreement. At low LO power, thermal noise dominates and the sensitivity cannot be noticeably improved even with very well matched path lengths (i.e., excellent CMRR). On the other hand, in the high LO power region, the system performance is dominated by the LO-RIN beat noise. Improved path length mismatch (i.e. improving CMRR) can result in great enhancement in the receiver sensitivity. For an optimized LO power of 11 dBm and a 2ps nominal P/N skew mismatch, -33dBm receiver sensitivity can be achieved with 112.8 Gb/s PM-QPSK signals at GFEC cliff. Another interesting observation from Fig. 5 (also predicted by Eq. (11)) is that for each LO power, and for a given thermal noise and RIN level, there exists a CMRR value beyond which the Rx sensitivity cannot be further improved. This corresponds to the condition when the sensitivity is dictated by the thermal noise impact.

6. Discussion

By introducing the concept of coherent receiver input referred noise variance, shot noise is no longer dependent on the LO power and acts as a constant noise floor. From Eq. (15), we can see the clear interplay of thermal noise, RIN, and CMRR on the performance of a balanced coherent receiver. If the thermal noise and the RIN levels are known for the TIA and laser, one can extract the average CMRR value by simply monitoring the optimum LO power. This provides a simple method to quantify the balancing quality of the coherent mixer in the optical front end. Also, from Eqs. (12) to (14), we see that all three noise terms are a function of the effective receiver bandwidth, which relates to the baud rate of the input signal. This means that the optimum LO power for best receiver sensitivity (varies with different bit rate) will be independent of the input signal data rate.

This paper is focused on the noise terms from the optical front end (OFE) of the coherent receiver. Detailed description of noise mechanisms inside the ADC/DSP circuits are beyond the scope of this paper. Here, we briefly discuss two noise sources interfacing the OFE and ADC/DSP that could potentially degrade the receiver sensitivity. The first one is the noise characteristics in the analog front end of the MODEM, namely the effective number of bits (ENOB) of the ADC. ENOB is not only a function of the frequency, but also a function of the input voltage swings. For high sensitivity applications, it is required that the TIA provides sufficient gain such that the input signal strength to the ADC is within the specification of the ENOB. The second noise source is the interplay of the LO phase noise with DSP. LO phase noise is taken care of by the digital carrier phase estimation. LO phase noise to amplitude noise conversion via the digital chromatic dispersion (CD) equalizer [10] acts more like a random noise floor onto the digital waveforms. This conversion strength is not only proportional to the transmission distance (i.e., the amount of CD being compensated), but is also proportional to the data rate [10]. Fortunately, with the bit rate and the distance of interest for unamplified applications, LO with < 1 MHz linewidth should have negligible impact on the sensitivity degradation. However, sensitivity degradation could be expected when the LO linewidth goes beyond several MHz.

7. Conclusion

A key advantage of coherent detection is its superior receiver sensitivity compared to direct detection. Therefore, coherent technologies have great potential for transmitting high data rates (100 Gb/s and beyond) over unamplified links. For this “dark fiber” application, we show, via analytical models and numerical simulations, that optimum receiver performance is achieved when the thermal noise is balanced with the residual LO intensity beat noise. This results in an optimum LO power for a given integrated coherent receiver. For a practical 100 Gb/s transmission, we show that a receiver sensitivity of -33 dBm is practical when the LO power is optimized. This translates to unamplified distances in excess of 100 km, depending on transmit optical power as well as the fiber loss. We also provide a simple method to monitor the imperfections of an integrated balanced receiver.